Deformation and failure of frozen soils and ice at constant and steadily increasing stresses

ANATOLY M. FISH

Office of the Federal Inspector of the Alaska Natural Gas Transportation System
and
U.S. Army Cold Regions Research and Engineering Laboratory, Box 282, Hanover, N.H. 03755, USA

Experimental and theoretical studies were made of the deformation and time-dependent failure of ice. Uniaxial compression tests were performed in the laboratory at constant and steadily increasing stresses. Strength criteria and unified constitutive equations describing all three stages of creep at constant stress are presented. It is shown that regardless of the stress regime (constant stress or step loading) the equations describe deformation and time-dependent failure by five parameters. The forms of the constitutive equations, which can be applied also to describe the mechanical properties of frozen and unfrozen soils, make it possible to obtain analytical solutions of the practical problems and to determine the creep parameters of frozen and unfrozen soils and ice *in situ*.

Des études expérimentales et théoriques ont été effectuées sur la déformation de la glace et sa rupture en fonction du temps. En laboratoire, ont été réalisés des essais de compression uniaxiale en présence d'efforts constants et augmentant régulièrement. Des critères de résistance mécanique et des équations détaillées uniformes sont présentés, décrivant les trois phases de fluage sous l'effet d'une contrainte constante. Il est démontré que, quel que soit le régime de contrainte (contrainte constante ou charge progressive), les équations décrivent la déformation et la rupture dépendante du temps au moyen de cinq paramètres. Les formes des équations détaillées que l'on peut aussi employer pour décrire les propriétés mécaniques des sols gelés ou non gelés, permettent de trouver des solutions analytiques aux problèmes pratiques et de déterminer les paramètres de fluage des sols gelés, des sols non gelés et de la glace *in situ*.

Proc. 4th Can. Permafrost Conf. (1982)

Introduction

It is known that frozen soils and ice exhibit pronounced rheological properties. These properties are expressed in the form of strength decrease, stress relaxation, and development of creep deformation with time. The strength and deformation characteristics of frozen soils and ice describing these properties depend upon the type of test, the rate of loading, and other factors. As a rule the rheological characteristics are determined from laboratory creep tests, which are time-consuming and costly. Determining the rheological characteristics *in situ* by means, for example, of pressuremeters does not eliminate the deficiencies of creep tests (Fish 1976; Ladanyi and Saint-Pierre 1978; Zaretskiy and Fish 1974*a* and *b*).

The rheological characteristics of frozen soils and ice can be determined from laboratory or field tests (Ladanyi and Johnston 1973) under monotonically increasing load or step loading. In this case, the constitutive equations and failure criteria established must reflect the behavior of frozen soils or ice under both constant loads and step loading. Moreover, the rheological properties of frozen soils and ice must be described by the same parameters. To do this the equations for various regimes must be derived on a unified theoretical basis. Also, to reduce the cost of testing, the number of parameters determined must be a minimum. Constitutive equations and failure criteria of such a type were derived (Fish 1976) and some results of their *practical* application are presented here. The *physical* aspects of frozen soil and ice deformation are not considered and are not referenced in the paper.

Experimental Studies

Experimental investigation of the deformation of ice as a function of time was carried out in a cold chamber, using freshwater lake ice. The blocks of ice destined for the experiments had a three-layered structure, with a total thickness $H \simeq 60$ cm. The two upper layers were cloudy, as they contained a large quantity of air bubbles. Samples for the tests were cut only from the lowest, transparent layer (about 20 cm thick), which contained practically no air inclusions. Crystallographic studies revealed that the ice in this layer had a columnar structure, the *C*-axes of the grains being oriented perpendicular to the freezing planes. The transverse dimensions of the crystals varied from 2.5 to 10 mm. Samples turned on a lathe were in the form of cylinders with a diameter $d = 50.5$ mm (area 20 cm^2), and a height of 100 mm. The generatrices of the cylinders were aligned parallel to the surface of freezing. The load was applied perpendicular to the *C*-axes of grains in the sample through rigid metal platens whose diameters matched the diameter of the sample. To avoid tilting and concentration of stresses while the load was being transmitted, the ends of the samples were smoothed on a polishing plate, while mounted in a foam plastic holder.

To study the influence on the test results of the conditions under which the ends of the samples were supported during the tests, three series of experiments were conducted to determine the "instantaneous" strength of the ice for different end conditions. The experiments were conducted in a hydraulic press in a cold chamber. Loading of the sample was such that failure ensued in 2 to 3 s. The ends of the samples of the first series were frozen to the platens (complete adhesion). In the second, the platens were placed against the samples without freezing and without lubrication (dry friction). In the third series, the surfaces of the platens were lubricated with cooled machine oil before being placed on the samples. Tests were performed at a constant temperature of -4 ± 0.2°C. The samples were kept at this temperature for at least 24 hours before the start of the test. The temperature was determined on the basis of a control sample with a mercury thermometer inserted in it. The test results are shown in Table 1.

For these experiments, which served only to establish test methodology, ice from the middle layer of the block was used. It is seen from the table that the application of the lubricant yielded the best reproducibility of the results; therefore, this treatment of the platens at the ends of the samples was used in all further tests.

TABLE 1. Failure load with different sample-platen conditions

Condition	Failure load, *kN*					
Frozen	14.8	8.9	5.3	5.1		
Dry friction	5.4	2.8	6.0	5.1	5.7	6.2
Lubricated	5.2	5.3	5.3	5.3	5.3	

In the main series of tests, which were performed on bubble-free ice, the nature of the failure of the samples was determined under rapid loading. Regardless of the method of treatment of the platens, splitting of the ice cylinders through the axis was observed in all cases. This fact indicates that with rapid loading there is a danger of transverse tensile strain which, on reaching a critical level, causes brittle failure of the ice as a result of cleavage in contrast to long-term viscous failure of the ice, controlled by shear mechanisms.

The "instantaneous" strength in compression of transparent ice was determined using the method set forth above. In a series of seven tests it was found that, in a direction parallel to the freezing surface, the average rupture stress $\sigma_0 \approx 2.56$ MPa with a relative error of $\pm$ 2.6 per cent. In a direction perpendicular to the freezing surface a slight anisotropy, $\sigma_\perp/\sigma_\parallel = 1.27$, was observed.

Experiments to discover the nature of deformation of ice as a function of time were performed on a lever-operated press set up in a cold-room. The axial deformation of the sample was measured with an ordinary dial-gauge extensometer. The temperature of the samples during the tests was kept at -4 ± 0.2°C. The experimental studies of the rheological properties of ice were performed under two loading regimes:

a) in creep, at constant stress, σ = constant
b) in step loading, $\sigma \simeq \dot{\sigma}t$.

In the creep experiments, the applied stress was fixed at certain levels below $\sigma_0 = 2.56$ MPa; the fractional multipliers of σ_0 were 0.9, 0.8, 0.6, 0.5, 0.4, 0.35, 0.25, 0.20, 0.10, and 0.05, giving stresses of 2.29, 2.04, 1.53, 1.275, 1.02, 0.89, 0.765, 0.64, 0.51, 0.25, and 0.15 MPa, respectively. In tests with step loading, the value of the increments in all cases was the same, $\Delta\sigma = 0.2$ MPa. The duration of the stress increments varied for different tests. The reproducibility of the results of the experiments was verified under step loading. Each of these tests were performed twice, and good agreement was found for all tests.

Short-Term Creep of Ice Under Constant Stress

Figure 1 shows the results of tests performed on ice in creep under the loading regime σ = constant. The special nature of short-term creep in ice is that the stage of secondary creep, i.e., a relatively long time interval during which the creep rate remains constant, is not reached. Accordingly, it is found that at stresses below or equal to the limit of long-term creep for ice ($\sigma \leqslant \sigma_\infty$), shear deformation builds up steadily at a decreasing rate, while at $\sigma > \sigma_\infty$ the first stage of creep makes a smooth transition to the third stage, characterized by an increase in the creep rate.

The decrease in the creep rate is due, above all, to the specific characteristics of the loading regime σ = constant, since in other types of test (for example $\sigma = \dot{\sigma}t$) a decrease in the creep rate was not observed.

From a physical point of view, the limit of long-term creep corresponds to the ultimate stress above which deformation of frozen soil or ice is accompanied by microcrack formation (Gold 1972). For frozen soils this limiting stress can be associated with the limit of the long-term strength of the soil. A curve of the ultimate strength (time-dependent failure) of ice is presented in Figure 2a.

An equation describing complete creep of ice at constant stress was presented in Zaretskiy and Fish (1974*a* and *b*). The derivation of the constitutive equations and the failure criteria of frozen soil or ice

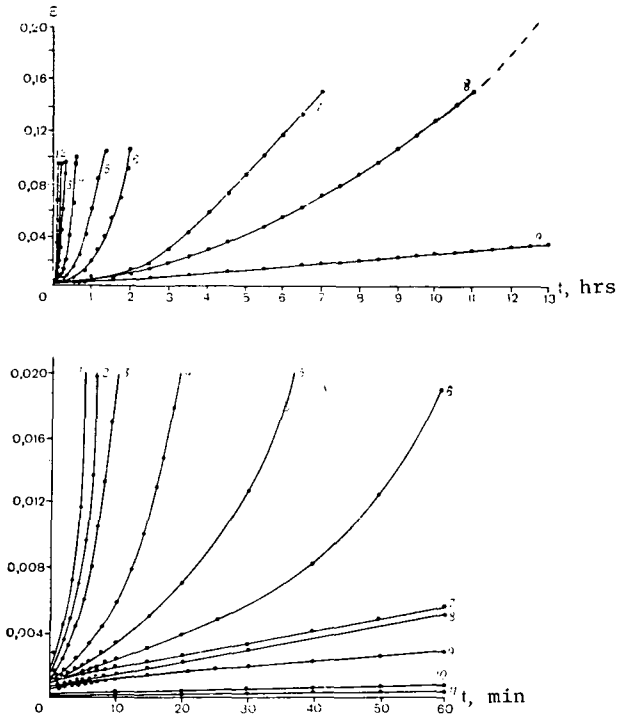

FIGURE 1. Creep curves of ice at stresses σ, in MPa, equal to the following: 2.295 (1); 2.04 (2); 1.53 (3); 1.275 (4); 1.02 (5); 0.89 (6); 0.765 (7); 0.64 (8); 0.51 (9); 0.25 (10); and 0.15 (11).

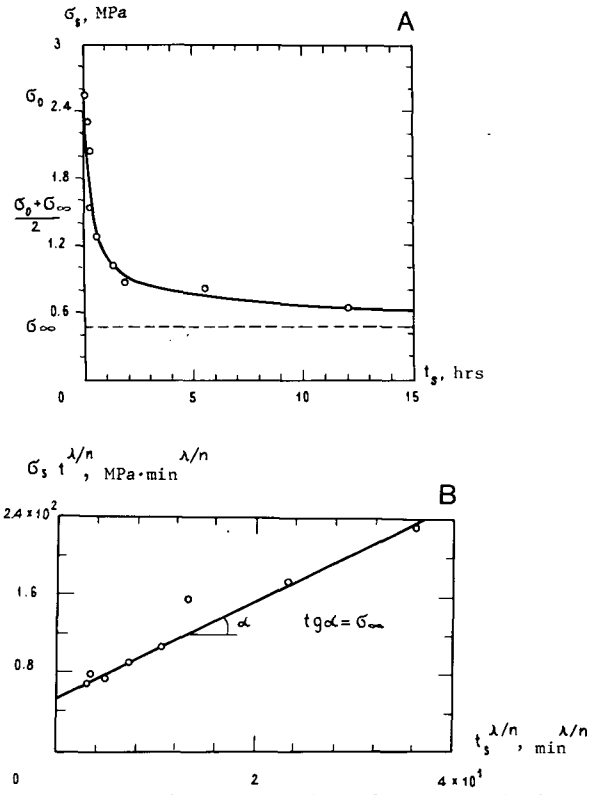

FIGURE 2.a Curve for long-term failure of ice. b Determination of parameters σ_∞ and $A^{1/n}$.

based upon the application of the kinetic theory of strength is presented in Fish (1976). The final equations convenient for analysis of the experimental data are presented below:

$$[1] \qquad \varepsilon^{(c)} = \varepsilon - \varepsilon^{(o)} = \frac{B\sigma^n t^\lambda}{A - (\sigma-\sigma_\infty)^n t^\lambda \eta(\sigma-\sigma_\infty)},$$

where ε, $\varepsilon^{(c)}$, and $\varepsilon^{(o)}$ are complete strain, creep strain, and instantaneous axial strain, respectively; A and B are parameters; n and λ are stress and time hardening parameters, respectively; and σ_∞ is the limit of the long-term strength. A function $\eta(\sigma-\sigma_\infty)$ is a unit function such that when $\sigma > \sigma_\infty$ the function $\eta \equiv 1$, and when $\sigma \leqslant \sigma_\infty$ the function η is identical to zero.

The relationship in equation 1 can be written in greater detail as follows:

$$[2] \qquad \varepsilon^{(c)} = \frac{B}{A}\sigma^n t^\lambda \qquad \text{for } \sigma \leqslant \sigma_\infty$$

$$[3] \qquad \sigma^{(c)} = \frac{B\sigma^n t^\lambda}{A - (\sigma-\sigma_\infty)^n t^\lambda} \qquad \text{for } \sigma > \sigma_\infty .$$

As mentioned above, at stresses greater than the creep limit σ_∞, the rate of flow of ice increases with time. Upon failure of the ice, the rate of flow increases rapidly toward an infinitely large value. On the basis of equation 1, one can conclude that the time to failure of the ice t_s is linked to the failure stress σ_s by the relationship.

$$[4] \qquad t_s = \frac{A^{1/\lambda}}{(\sigma_s-\sigma_\infty)^{n/\lambda}}$$

or

$$[5] \qquad \sigma_s = \sigma_\infty + \frac{A^{1/n}}{t_s^{\lambda/n}} .$$

The latter is a criterion of the time-dependent failure of ice, which was used to analyze the experimental data (*see* Figures 1 and 2). Some results of this analysis were published earlier. A complete analysis of the test data is presented in Fish (1976).

Short-Term Creep of Ice at Steadily Increasing Stresses

In tests under a step increase type of loading, the value of each stress increment was equal to $\Delta\sigma$ = 0.2 MPa but the duration of the stress increments varied. Thus, in the first series of tests it was two minutes, in the second series it was five minutes, in the third series, ten minutes, and finally in the fourth

series, thirty minutes. The results of these tests are shown in Figures 3 and 4.

Even a cursory analysis of the experiments (*see* Figure 4) shows the clear validity of the assumption that, in the case of a monotonically increasing load, the first stage of creep will be absent. At stresses $\sigma(t)$ less than or equal to a certain limit $\xi\sigma_\infty$, where $\xi \geqslant 1$ is a multiple of the long-term creep limit σ_∞, the creep rate will increase monotonically as the stresses rise, and at stresses above this limit, the creep rate will accelerate. It is interesting to note that it was found theoretically that the value of ξ is approximately 2, and is equal to the sum of n and λ.

A complete set of constitutive equations and failure criteria describing these tests was derived in the work of Fish (1976). The derivation was based upon the expansion of the rate process theory (kinetic theory of strength), applied originally for creep at constant stresses, to the range of monotonically increasing stresses.

The final constitutive equation for step loading has the following form:

$$[6] \qquad \varepsilon^{(c)} = \varepsilon - \varepsilon^{(o)} = \frac{2B\dot{\sigma}^n t^{\lambda+n}}{2A - (\dot{\sigma}t - 2\sigma_\infty)^n t^\lambda \eta(\dot{\sigma}t - 2\sigma_\infty)},$$

where the hardening parameters are $n \geqslant 1$; $\lambda \leqslant 1$; $n + \lambda \approx 2$.

Here $\eta(\dot{\sigma}t - 2\sigma_\infty)$ is the unit function such that when $\dot{\sigma}t > 2\sigma_\infty$, $\eta = 1$, and when $\dot{\sigma}t \leqslant 2\sigma_\infty$ the function η is equal to zero. The rest of the parameters have the same meanings as in the case of creep under constant stresses.

The relationship in equation 6 can be written in greater detail as follows:

$$[7] \qquad \varepsilon^{(c)} = \frac{B}{A}\dot{\sigma}^n t^{\lambda+n} \qquad \text{for } \sigma(t) < 2\sigma_\infty$$

and

$$[8] \qquad \varepsilon^{(c)} = \frac{2B\dot{\sigma}^n t^{\lambda+n}}{2A - (\dot{\sigma}t - 2\sigma_\infty)^n t^\lambda} \qquad \text{for } \sigma(t) > 2\sigma_\infty.$$

As we pointed out earlier, at stresses $\sigma(t) > 2\sigma_\infty$ the flow rate of ice increases with time. Upon the failure of ice, the flow rate tends toward an infinitely large value. Based upon equation 6, one can conclude that the time to failure of the ice t_s is linked to the failure stress $\sigma_s \approx \dot{\sigma}_s t_s$ by the relationship

$$[9] \qquad t_s = \frac{2A}{\dot{\sigma}t_s - 2\sigma_\infty}$$

if it is assumed that the stress and the time hardening have little effect upon the time-dependent failure of ice under monotonically increasing stresses.

To analyze the results of the experiments, we approximated the step loading as a monotonically increasing compressional stress in accordance with the law $\sigma(t) \simeq \dot{\sigma}t$. Thus, in the first case the rate of loading was $\dot{\sigma} = 0.1$ MPa/min, in the second, $\dot{\sigma} = 0.04$ MPa/min, in the third $\dot{\sigma} = 0.02$ MPa/min, and in the fourth $\dot{\sigma} = 0.0067$ MPa/min. Since the deformation ε of the ice sample at each stage of the loading has an "instantaneous" component $\varepsilon^{(o)}$ (*see* Figure 4), this part of the deformation was eliminated in order to determine the parameters that characterize the creep process in the ice (Figure 5), and in the figures presented below the deformations are shown as $\varepsilon^{(c)} = \varepsilon - \varepsilon^{(o)}$. For approximating the test results under step loading as test results under monotonically $\sigma = \dot{\sigma}t$, we used deformations and strain rates corresponding to the final stages of loading (Figures 6 and 7) in the analysis of the experimental data.

At a low stress level $\sigma(t) < 2\sigma_\infty$, the experimental data in logarithmic co-ordinates "$\ln\sigma - \ln\varepsilon^{(c)}$" will consist, according to formula 7 and also equation 13,

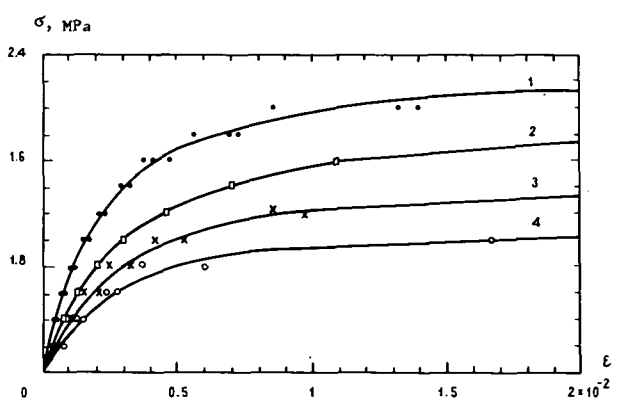

FIGURE 3. Relationship σ vs. ε for step loading with a stress step value of $\Delta\sigma = 0.2$ MPa for a duration of loading t, equal to 2 (1), 5 (2), 10 (3), and 30 (4) min.

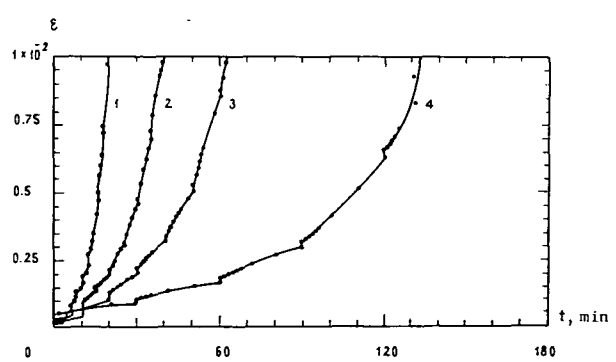

FIGURE 4. Relationship ε vs. t for step loading with a stress step value $\Delta\sigma = 0.2$ MPa and durations of loading t of 2 (1), 5 (2), 10 (3), and 30 (4) min.

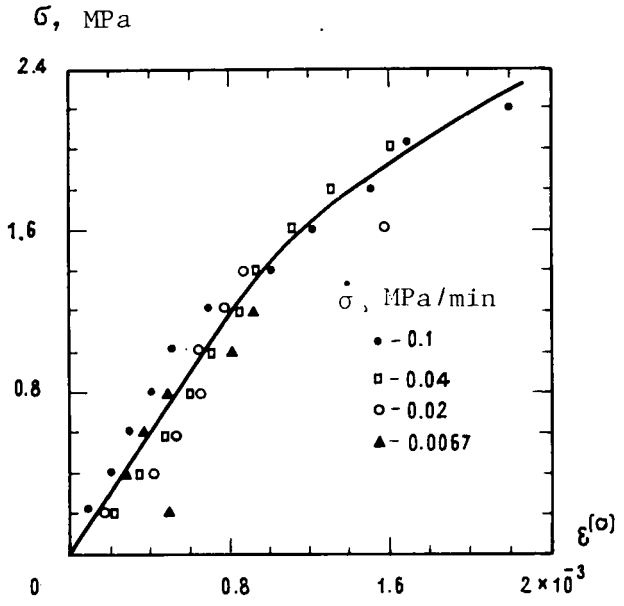

FIGURE 5. Relationship σ vs. $\varepsilon^{(\sigma)}$ for step loading.

of a family of parallel straight lines, for which the tangent of the slope angle with the axis "$\ln\sigma$" will be equal to value of $(n + \lambda)$. Figure 8 shows such a plot. The value of $(n + \lambda)$ turned out to be 1.85, which agrees well with the theoretically predicted value of 2. In Figure 8**b**, the co-ordinates "$\ln\varepsilon_0^{(c)}$ vs. $\ln\dot{\sigma}$" have been used to plot the values of the segments intersected by a family of curves on the "$\ln\varepsilon^{(c)}$" axis (Figure 8**a**) as a function of the rate of loading. The value of parameter $\lambda = 0.7$, equal to the tangent of the angle formed by the straight line thus obtained and the "$\ln\dot{\sigma}$" axis. The value of the intercept on the vertical axis is equal to the strain hardening modulus $B/A = 1.5 \times 10^{-4}$ (MPa)$^{-n}$/min$^{\lambda}$ while the deformation modulus $E_0 = 1400$ MPa (*see* Figure 5).

Failure of ice samples in step loading occurred just as in the conditions of creep at constant stress and corresponded to a time when the strain rate tended toward infinity. The moment of failure in all of the experiments corresponded to a deformation of ≈10 per cent (*see* Figure 7), when the tangents to the "$\varepsilon^{(c)} - t$" curves approached vertical. The time to failure t_s depended significantly upon the rate of loading $\dot{\sigma}$. Figure 9**a** shows this relationship. As predicted by strength criterion 9, a high rate of loading gives a shorter time to failure. These results are in agreement with the data of Vyalov and Chernigov (1960). Taking into account the fact that the parameter n differs only slightly from unity and parameters $(n + \lambda)$ only slightly from 2, then in determining the strength characteristics, strength criterion 9 can be used. For this purpose, one replots the relationship t_s $(\dot{\sigma})$ in "$\dot{\sigma}_s t_s^2/2$ vs. t_s" co-ordinates; in this graph (Figure 9**b**) the experimental data should plot as a straight line. The tangent of the slope angle with respect to the abscissa will be equal to the value of the long-term creep limit of ice, $\sigma_\infty = 0.48$ MPa. The intercept on the vertical axis gives the value of parameter $A = 18.1$ MPa/min. Finally, one can determine the value of parameter $B = 2.7 \times 10^{-3}$. For comparison, a method for determining the parameters A and σ_∞ from the tests at σ = constant is given (*see* Figure 2**b**).

Thus, all the parameters that enter into constitutive equation 7 and failure criterion 9 were determined and show a good agreement with the results of the foregoing analysis of the stress regime σ = constant. (Zaretskiy and Fish 1974*a* and *b*).

Hence it can be concluded that the constitutive equation characterizing the relationship between deformation, loading rate, and time under mono-

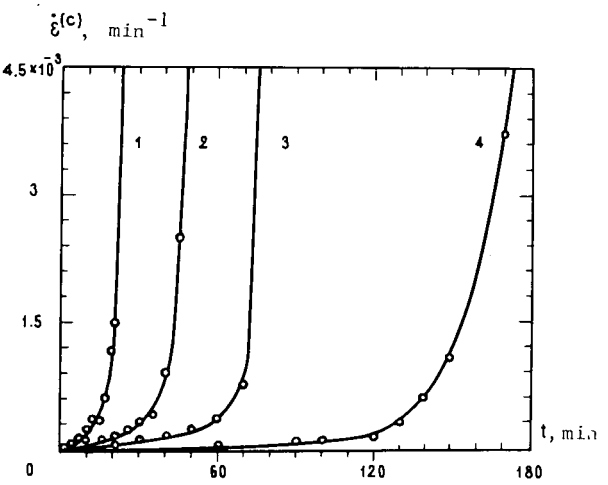

FIGURE 6. Relationships $\dot{\varepsilon}^{(c)}$ vs. t for step loading at the following rates of loading $\dot{\sigma}$ in MPa/min: 0.1 (1); 0.04 (2); 0.02 (3); 0.0067 (4).

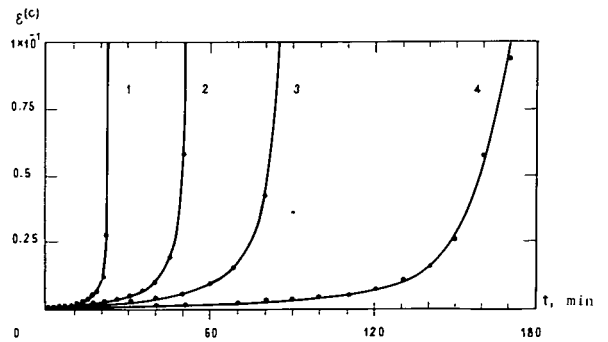

FIGURE 7. Relationships $\varepsilon^{(c)}$ vs. t for step loading at the following rates of loading $\dot{\sigma}$ in MPa/min: 0.1 (1); 0.04 (2); 0.02 (3); 0.0067 (4).

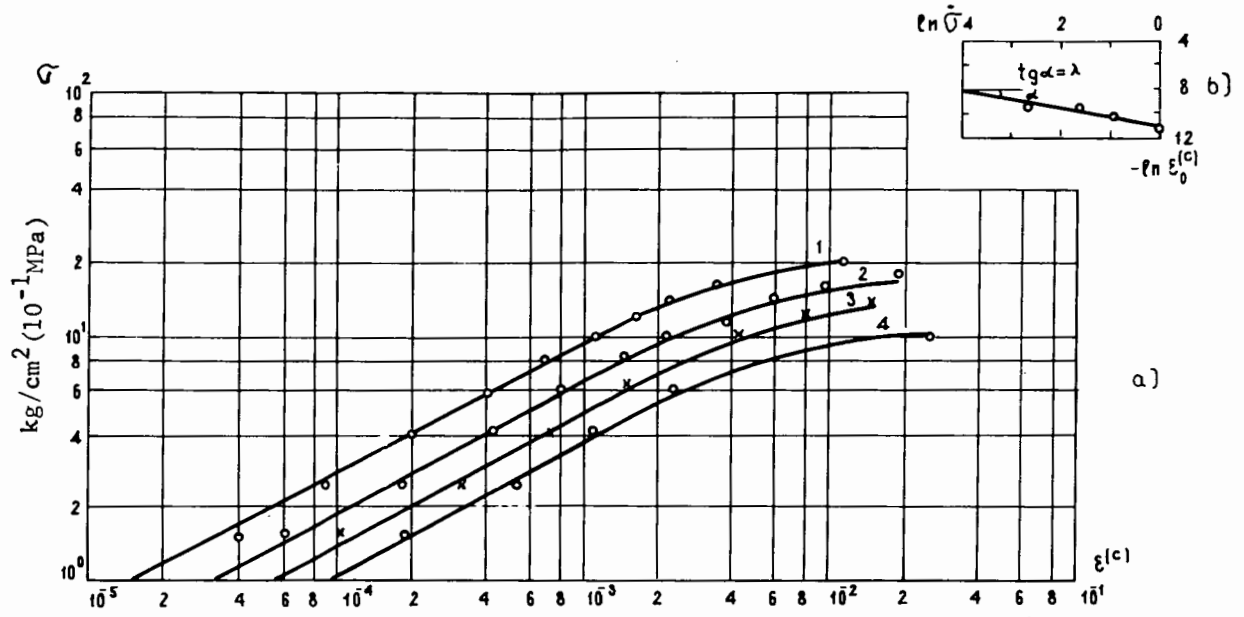

FIGURE 8. Relationships σ vs. $\varepsilon^{(c)}$ for step loading in logarithmic co-ordinates at the following rates of loading $\dot{\sigma}$ in MPa/min: 0.1 (1); 0.04 (2); 0.02 (3); 0.0067 (4).

tonically increasing load (actually step loading) and the criterion for long-term strength, fit the experimental data.

It remains to verify the general relationship 8, which is valid for $\sigma(t) > 2\sigma_\infty$. A verification of this equation will consist of showing the correspondence of the experimental data with the equation, and the correspondence of parameters n, λ, and B/A, determined earlier on the basis of experimental data with $\sigma(t) < 2\sigma_\infty$. For this purpose, relationship 8 can be rewritten as follows:

$$[8a] \qquad \frac{\dot{\sigma}^n t^{\lambda+n}}{\varepsilon^{(c)}} = \frac{A}{B} - \frac{1}{2B}(\dot{\sigma}t - 2\sigma_\infty)^n t^\lambda .$$

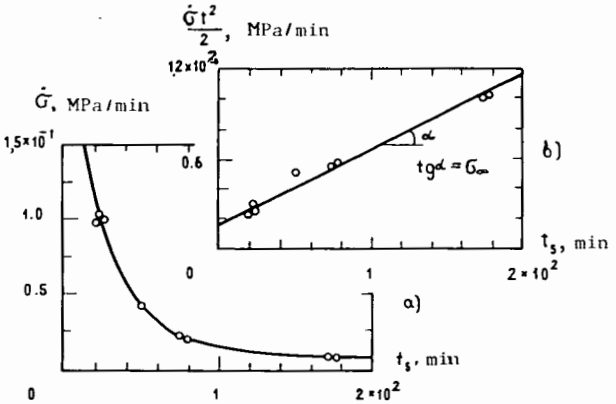

FIGURE 9.a Loading rate $\dot{\sigma}$ vs. time to failure t_s; and b determination of parameters σ_∞ and A.

If we then plot all the experimental data on a graph in the co-ordinates "$\dot{\sigma}^n t^{\lambda+n}/\varepsilon^{(c)}$ vs. $(\dot{\sigma}t - 2\sigma_\infty)^n t^\lambda$," using values of parameters n and λ from the foregoing analysis for the plot, the result will be a straight line. The cotangent of the slope angle with respect to the abscissa determines the double value of parameter B. The intercept with the vertical axis is equal to the value of the ratio A/B. Figure 10 shows this construction, giving values of parameter $B = 2.3 \times 10^{-3}$ and the ratio $B/A = 1.7 \times 10^{-4}$ (MPa)$^{-n}$/min$^{\lambda}$. (The correlation coefficient $K_1 = 0.91$, and the dispersion $K_2 = 0.72$.) According to data obtained earlier with $\sigma(t) < 2\sigma_\infty$, the ratio $B/A = 1.5 \times 10^{-4}$ (MPa)$^{-n}$/min$^{\lambda}$ from which parameter $B = 2.7 \times 10^{-3}$. In this plot the stress has dimensions of kg/cm^2.

The investigations described above permit the conclusion that the proposed constitutive equations and failure criteria are in agreement with experimental data, and can be used to describe rheological processes in ice over the *entire* range of monotonically increasing compressive stresses.

Some Generalizations

Studies of deformation and failure of ice have shown that the proposed constitutive equations conform with the experimental data over the entire range of constant stresses and stresses that increase slowly with time. The rheological properties of ice are described by five parameters: n, λ, and B, which are dimensionless parameters; σ_∞, which is the long-term

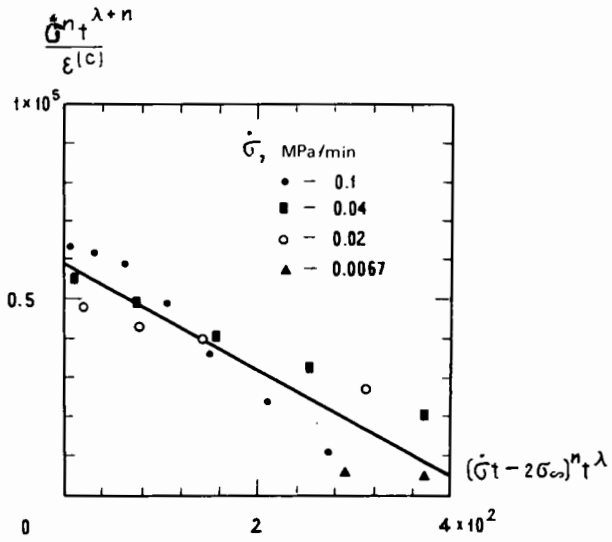

FIGURE 10. Analysis of relationship

$$\varepsilon^{(c)} = \frac{2B\sigma^n t^{\lambda+n}}{2B - (\dot{\sigma}t - 2\sigma_\infty)^n t^\lambda} \qquad \text{for } \dot{\sigma}t > 2\sigma_\infty.$$

creep limit of ice, and finally A, which is a generalized parameter. The correspondence between the rheological constants determined by both loading regimes has been demonstrated. To show that this close correspondence is not accidental, consider three variants of the creep theory according to Zaretskiy and Fish (1974*a* and *b*) that give different results for the predicted deformation under time-dependent loading regimes. However, all theories give equivalent results for constant stresses. The relationships among deformation, stress, and time for the theories of aging, flow, and creep in terms of stress history, taking into account the circumstance that at σ = constant for all of these theories, lead to the result expressed by formula 2 for $\sigma < \sigma_\infty$. These relationships can be written as:

Theory of aging

$$[10] \qquad \varepsilon^{(c)} = \frac{B}{A}\sigma^n(t)t^\lambda$$

Theory of flow

$$[11] \qquad \varepsilon^{(c)} = \frac{B}{A}\lambda \int_0^t \sigma^n(\tau)\tau^{\lambda-1}d\tau$$

Theory of creep in terms of stress history

$$[12] \qquad \varepsilon^{(c)} = \frac{B}{A}\lambda \int_0^t \frac{\sigma^n(\tau)\,d\tau}{(t-\tau)^{1-\lambda}} .$$

It can be seen that all of these formulas, when σ = constant, give the same result. Substituting $\sigma = \dot{\sigma}t$ in the formulas presented above gives, after rearranging, the following expression:

$$[13] \qquad \varepsilon^{(c)} = \varkappa \frac{B\sigma^{n+\lambda}}{A\dot{\sigma}^\lambda} .$$

Here the parameter $\varkappa$ is given the following values:

In the theory of aging $\varkappa_I = 1$,
In the theory of flow $\varkappa_{II} = \lambda/(n+\lambda)$
In the theory of creep
in terms of stress history

$$[14] \qquad \varkappa_{III} = \frac{\lambda}{n+\lambda} \cdot \frac{\Gamma(n+1)\Gamma(\lambda)}{\Gamma(n+\lambda+1)}$$

where $\Gamma(x)$ is the gamma function.

By comparing the resultant value for the parameter $\varkappa$ with theoretical values $\varkappa_I = 1$; $\varkappa_{II} = 0.35$; and $\varkappa_{III} = 0.25$, one concludes that the deformation theory of aging, in regimes of monotonically increasing load, best corresponds to the experimental results of the investigation of rheological processes occurring in ice during uniaxial compression. Relationship 13 also predicts the possibility of strain hardening for monotonic loading. In the absence of the latter, the sum of the parameters $n + \lambda = 2$ according to equation 6. Using experimental data even with a step increase in the load, $n + \lambda = 1.85$. Therefore the conclusion reached earlier, namely that the influence of strain hardening and restoration of the bonds upon the durability (long-term strength) of ice under monotonic increase in stress in conditions of short-term creep is not very perceptible, is confirmed by the experimental data and is justified.

The agreement between the values of the rheological parameters determined by the two methods makes it possible to recommend the method of monotonic (actually step) loading as being the most effective for *practical use* in determination of the rheological properties of ice. This method makes it possible to reduce the time and effort involved in determining the rheological parameters by a factor of at least eight in comparison with ordinary creep tests at constant stresses.

The extent to which the rheological parameters determined by the two methods correspond to the experimental data can be demonstrated. Figures 11 and 12 show the theoretical and experimental creep curves of ice in step loading, with different rates of stress increase. Note that when plotting the theoretical curves in accordance with constitutive equations 7 and 8, the values of the rheological parameters determined from creep tests under the loading regime of σ = constant were used. The theoretical and experimental curves for long-term strength of ice obtained in tests using the two methods are shown in Fig-

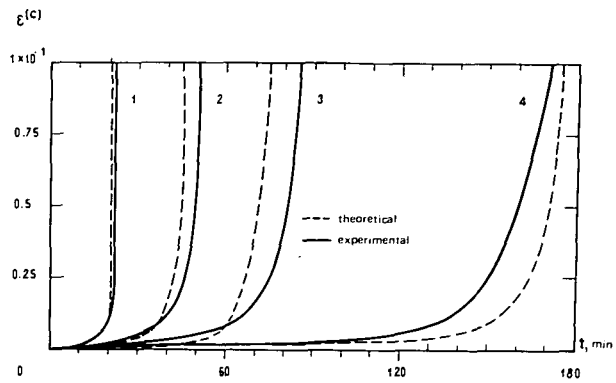

FIGURE 11. Theoretical and experimental relationships $\varepsilon^{(c)}$ vs. t for step loading at the following rates of loading $\dot{\sigma}$ in MPa/min: 0.1 (1); 0.04 (2); 0.02 (3); and 0.0067 (4).

ure 13. In this case, on the contrary, the values for the rheological parameters were used which were determined from tests under the loading regime $\sigma(t) = \dot{\sigma}t$ in plotting the theoretical relationships in accordance with the failure criteria 4 and 5. There is good agreement between the theoretical and experimental curves.

The results of tests on creep of ice under uniaxial compression enable one to formulate constitutive equations valid for various stress states. Keeping in mind that, for active loading regimes resembling monotonically increasing stress, the deformation theory of aging leads to acceptable results, equations of the type of 1 and 6 can be applied to the case of the complex stress state. Under the regime of loading σ_i = constant:

$$[15] \quad \varepsilon_i^{(c)} = \frac{B_i}{A_i}\sigma_i^n t^\lambda \qquad \text{for } \sigma_i < \sigma_{i(\infty)}$$

and

$$[16] \quad \varepsilon_i^{(c)} = \frac{B_i \sigma_i^n t^\lambda}{A_i - (\sigma_i - \sigma_{i(\infty)})^n t^\lambda} \qquad \text{for } \sigma_i > \sigma_{i(\infty)}.$$

Under the regime of step loading $\sigma_i(t) \simeq \dot{\sigma}_i t$.

$$[17] \quad \varepsilon_i^{(c)} = \frac{B_i}{A_i}\dot{\sigma}_i^n t^{\lambda+n} \qquad \text{for } \sigma_i(t) < 2\sigma_{i(\infty)}$$

and

$$[18] \quad \varepsilon_i^{(c)} = \frac{2B_i \dot{\sigma}_i^n t^{\lambda+n}}{2A_i - (\dot{\sigma}_i t - 2\sigma_{i(\infty)})^n t^\lambda} \qquad \text{for } \sigma_i(t) > 2\sigma_{i(\infty)}.$$

Here σ_i is the octahedral shear stress; $\varepsilon_i^{(c)}$ is the octahedral shear creep strain. Values of parameters n and λ are identical to those determined from tests in uniaxial compression. The ratio A_i/B_i, the ratio A/B determined from experiments under uniaxial compression, is as follows:

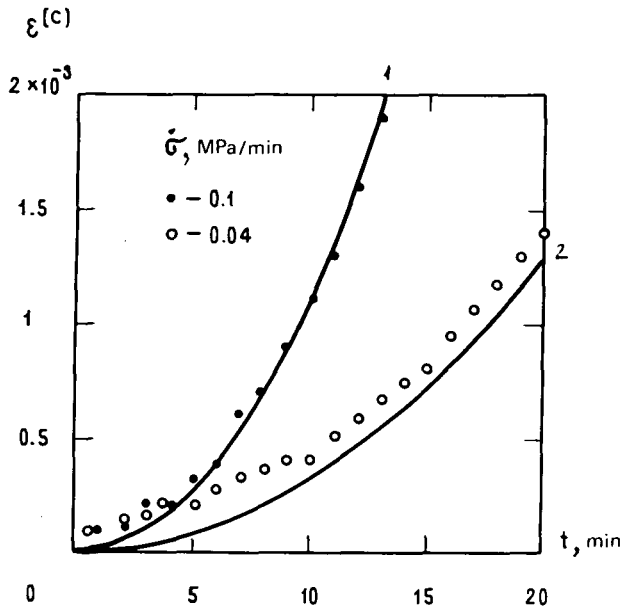

FIGURE 12. Theoretical and experimental relationships $\varepsilon^{(c)}$ vs. t for the rates of loading $\dot{\sigma}$ in MPa/min of 0.1 (1) and 0.04 (2) (initial segments of curves).

$$[19] \quad \frac{A_i}{B_i} = 3^{-\frac{n+1}{2}} \frac{A}{B}.$$

Equations 15 to 18 can be used to describe the deformation and failure of other materials, especially frozen and unfrozen soils. In the latter case, $\sigma_{i(\infty)}$ will have the meaning of the long-term strength limit in a complex stress state; according to the hypothesis of von Mises and Schleicher it can be represented in the form

$$[20] \quad \sigma_{i(\infty)} = c_\infty + \sigma_{oct} \tan\phi.$$

where σ_{oct} is the octahedral stress.

In the case when the angle of internal friction of the soil $\phi = 0$, $\sigma_{i(\infty)} = \sigma_\infty/3^{1/2}$, where σ_∞ is the long-term strength limit in uniaxial compression.

Constitutive equations 15 to 18 were used to determine the rheological parameters of ice *in situ* by means of a pressuremeter. These equations can also be used for the solution of problems on the stress–strain state of tunnels, and for the determination of the bearing capacity and deformability of ice fields, foundations of buildings, airport runways, roads, stream crossings, and many other structures for which the underlying materials include frozen soils and ice.

Conclusion

To expand slightly on the physical and historical background of this work, the analytical forms of equations 1 and 6 were selected deliberately to make it possible to obtain closed analytical solutions of the

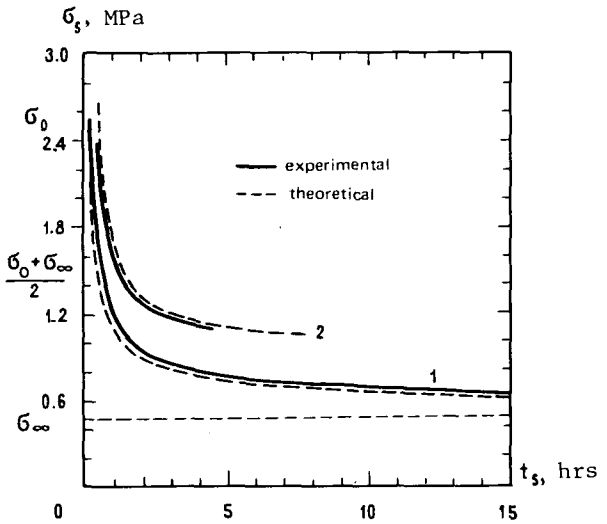

FIGURE 13. Theoretical and experimental curves for the long-term failure of ice under the following test conditions:

Creep tests σ = constant (1)
Step loading $\sigma(t) \simeq \dot{\sigma} t$ (2).

specific boundary problems. Initially, prior to expanding in the series and integrating, they had the following differential forms (Fish 1976):

$$[3a] \quad \dot{\varepsilon}^{(c)} = \lambda \frac{B}{A} \sigma^n t^{-\delta} e^{\delta t/t_s} \quad \text{for } \sigma = \text{constant}$$

$$[6a] \quad \dot{\varepsilon}^{(c)} = (\lambda + n) \frac{B}{A} (\dot{\sigma} t)^n t^{-\delta} e^{\delta t/t_s} \text{ for } \sigma(t) \approx \dot{\sigma} t$$

where $A = t_0^{\lambda} (\sigma_0 - \sigma_\infty)^n$, t_0 is the relaxation time, and $\delta = 1 - \lambda$.

These equations describe short-term creep of soils and ice better than equations 3 and 6. However, to obtain closed analytical solutions using them is very difficult. A remarkable property of equation 3*a* is that this accurately describes all three stages of a typical creep curve. According to equation 3*a*, a creep curve has an inflection point when $t = t_s$. The major components of these equations are the exponential terms $e^{\delta t/t_s}$, where the ratios δ/t_s are *functions*, describing curves of the long-term failure, not parameters or *points* at creep curves. Assuming that $n = 1$ and $\lambda B/A = 1/\eta$, where η is a viscosity coefficient, the function $t_s = T_p/\bar{\sigma}$, which is Zaretskiy's failure equation, and equation 3*a* will transform to the equation presented in Vyalov *et al.* (1973) and Zaretskiy *et al.* (1975) which was derived from different theoretical premises. In this the authors showed that their equation describes all three stages of creep and time-dependent failure and (if $n \simeq 1$) fits test data for frozen and unfrozen soils under simple and complex stress-strain states.

The general analytical forms of the exponential term

$$e^{\delta t/t_s},$$

which expresses the change of the entropy, were derived in (Fish 1976, 1980) from different theoretical premises. It was shown that they are valid for failure equations t_s at certain loading regimes. This was proven for the step loading regime (equations 6 and 6*a*) in which the function t_s is different. It was shown that the equations presented above describe not only complete creep of ice, but also the acoustic emission and recrystallization processes in ice during creep, and that the acoustic emissions can be used to predict time-dependent failure of a material.

In later work, earlier concepts were extended; both deformation and failure were considered to be a unified kinetic process, that takes place at the very start of deformation. A more general form of equation 3*a* presented by Fish (1980), that describes a complete creep process, has a substantially better analytical form then equations 3*a* and 6*a*:

$$[21] \quad \dot{\varepsilon} = \frac{C}{t_m} \left(\frac{\sigma}{\sigma_0}\right)^{\alpha} \left(\frac{t_m}{t}\right)^{\delta} e^{\delta t/t_m}.$$

In equation 21, C, α, and $\delta \leqslant 1$ are dimensionless parameters. This equation is based upon the failure criterion given by equation 22, assuming that $t_m \equiv t_s$ and $\sigma_\infty = 0$

$$[22] \quad t_m = t_0 \exp\left(m \frac{\sigma_0 - \sigma}{\sigma}\right) \approx t_0 \left(\frac{\sigma}{\sigma_0}\right)^{-m}; t_0 = \frac{h}{kT} e^{U/kT}$$

where σ_0 is the pseudo-instantaneous strength, t_0 is Frenckel's relaxation time, m is a parameter, U is the activation energy, k is Boltzmann's constant, h is Planck's constant, T is the absolute temperature K, and $\dot{\varepsilon}$ is the total strain rate. For step loading, the constitutive equation is equivalent to equations 21 and 6*a*, but the failure criterion is different.

Complete Short-Term Creep

Substituting equation 22 into equation 21 the latter becomes:

$$[23] \quad \dot{\varepsilon}^{(c)} = \dot{\varepsilon}_0 t^{-\delta} e^{\delta t/t_m}$$

or

$$[23a] \quad \varepsilon^{(c)} = \varepsilon - \varepsilon^{(o)} = B_1 \sigma^n t^{\lambda} e^{\delta t/t_m}$$

where

$$[24] \quad \dot{\varepsilon}_0 = A_1 \left(\frac{\sigma}{\sigma_0}\right)^n; A_1 = \frac{C}{t_0} \left(\frac{t_0}{t_*}\right)^{\delta}; B_1 = C/t_0^{\lambda} \sigma_0^n \lambda$$

ε_0 and $\dot{\varepsilon}_0$ are the strain and the strain rate at the time of loading when $t = t_* = 1$ min, $n = \alpha + m - m\delta$, and $\delta = 1 - \lambda$, (t_* can be omitted). Equation 23*a* is an approximate equation for creep deformations.

Secondary Creep

Strain rate reaches a minimum when $t = t_m$; after that the strain rate accelerates, i.e., when $t = t_m$, $\dot{\varepsilon} = \dot{\varepsilon}_m$, and $\varepsilon = \varepsilon_m$, equations 21 and 23 become:

$$[25] \quad \dot{\varepsilon}_m^{(c)} = \frac{C}{t_m}\left(\frac{\sigma}{\sigma_o}\right)^{\alpha} e^{\delta} = A_2 \left(\frac{\sigma}{\sigma_o}\right)^{\alpha_1} = \frac{\dot{\varepsilon}_o}{t_m^{\delta}} e^{\delta}$$

where $\alpha_1 = \alpha + m$; $A_2 = Ce^{\delta}/t_o$. From equations 21 to 25 it follows that:

$$[25a] \quad \dot{\varepsilon}_m^{(c)} = Ce^{\delta}\frac{kT}{h}\exp\left(-\frac{U}{kT}\right)\left(\frac{\sigma}{\sigma_o}\right)^{\alpha_1}$$

and

$$[25b] \quad \varepsilon_m^{(c)} = \dot{\varepsilon}_m^{(c)} t_m/\lambda.$$

Equation 25*b* is in agreement with Ladanyi's criterion (1972). The time functions of equation 21 are close to Assur's equation (1980).

Determination of Parameters

One test for σ_o and two creep tests are required to determine all five parameters t_o, m, C, n, and δ. First, creep curves are plotted in "$\ln\dot{\varepsilon}$ vs. $\ln t$" co-ordinates, that give values of $\dot{\varepsilon}_m$, t_m, and $\dot{\varepsilon}_o$. Parameters m and t_o are obtained plotting the values of t_m and the ratios σ/σ_o in co-ordinates "$\ln t_m$ vs. $\ln \sigma/\sigma_o$" (*see* equation 22). Then plotting the ratios of $\dot{\varepsilon}_o/\dot{\varepsilon}_m$ for given values t_m in co-ordinates "$\ln(\dot{\varepsilon}_o/\dot{\varepsilon}_m)$ vs. $\ln t_m$", the value of δ is obtained (*see* equations 24 and 25). Finally, plotting the values of $\dot{\varepsilon}_m$ for given t_m in co-ordinates "$\ln(\dot{\varepsilon}_m t_m)$ vs. $\ln(\sigma/\sigma_o)$", the parameters C and n are obtained. A method for determining the parameters of equation 23*a* using isochronous creep curves (Fish 1976) is very simple and is similar to that presented above.

The validity of equations 21 to 25*b* to test data on *short-term creep* of frozen and unfrozen soils at confined compression and the complex stress-strain state was demonstrated by the author at recent CRREL technical meetings. The complete theory with experimental data will be published in the near future. However, for *long-term creep* other models may be more suitable (Andersland and AlNouri 1970; Ladanyi 1972; Sayles 1974; and others).

However, the physical significance of the unified constitutive equations presented above extends far beyond a simple description of three stages of creep and time-dependent failure for practical purposes. Being based upon the Kinetic Theory of Strength (Rate Process Theory) they describe the *deepest* physical processes of deformation: the micro-crack formation and acoustic emission from frozen and unfrozen soils and recrystallization processes in ice (Fish 1976; Fish and Sayles 1981; Gold 1972; Vyalov *et al.* 1973; Zaretskiy *et al.* 1975; and others).

Acknowledgements

This work was performed under Contract No. DAAG 29-77-0016 between the Civil Engineering Department of the Massachusetts Institute of Technology and the U.S. Army Research Office. Appreciation is extended to Dr. A. Assur who supported the present studies and made valuable comments.

References

ANDERSLAND, O.B. AND ALNOURI L. 1970. ASCE Journal of Soil Mechanics and Foundation Div., Amer. Soc. Civil Eng., vol. 96, no. 4, pp. 1249–1265.

ASSUR A. 1980. Some promising trends in ice mechanics. IUTAM Symp. Copenhagen: Springer-Verlag, Berlin and Heidelberg.

FISH, A.M. 1976. An acoustic and pressuremeter method for investigation of the rheological properties of ice. Ph.D. thesis, Arctic and Antarctic Research Institute, Leningrad, USSR [Transl. from Russian]. U.S. Army Cold Regions Res. Eng. Lab., 1978 (*in press*).

———. 1980. Kinetic nature of the long-term strength of frozen soils. Preprints of the 2nd Int. Symp. Ground Freezing, Univ. Trondheim, Norway, pp. 99–108.

FISH, A.M. AND SAYLES, F.H. 1981. Acoustic emissions during creep of frozen soils. Acoustic Emissions in Geotechnical Engineering Practice, ASTM STP 750, V.P. Drnevich and R.E. Gray, Eds., Amer. Soc. Testing and Materials, pp. 194–205.

GOLD, L.W. 1972. The failure process in columnar-grained ice. Natl. Res. Counc. Can., Div. Build. Res., Technical Paper N369.

LADANYI, B. 1972. Engineering theory of creep of frozen soils. Can. Geotech. J., vol. 9, pp. 63–80.

LADANYI, B. AND JOHNSTON G.H. 1973. Evaluation of in-situ creep properties of frozen soils with the pressuremeter. Proc. 2nd Int. Conf. on Permafrost, North Amer. Contrib., pp. 310–318.

LADANYI, B. AND SAINT-PIERRE, R. 1978. Evaluation of Creep Properties of Sea Ice by Means of a Borehole Dilatometer. Proc., IAHR Symp. on Ice Problems, Lulea, Sweden, 1978, Part 1, pp. 97–115.

SAYLES, F.H. 1974. Triaxial constant strain rate tests and triaxial creep test on frozen Ottawa sand. CRREL Technical Report 253.

VYALOV, S.S., *et al.* 1973. Kinetics of structural deformation and failure of clays. Proc. 8th Int. Conf. Soil Mech. and Found. Eng., vol. 1, Moscow.

VYALOV, S.S. 1978. Rheological fundamentals of soil mechanics (in Russian). Vysshaya Skhola, Moscow.

VYALOV, S.S. AND CHERNIGOV, V.A. 1960. Stress and strain dependency of ice. Trans. Soviet Antarct. Exped. 2nd Cont. Exped., vol. 10 [in Russian]. Izd-vo Morskoy transport. Leningrad, 1960.

ZARETSKIY, YU. K. AND FISH, A.M. 1974*a*. Laws of ice deformation in time for uniaxial compression. AANII, Tr. 324:162-171 [In Russian], Gidrometeoizdat, Leningrad.

———. 1974*b*. Determination of the rheological properties of ice by means of a pressure meter. AANII, Tr. 324 [In Russian], Gidrometeoizdat, Leningrad.

ZARETSKIY, YU. K., FISH, A.M., GAVRILO, V.P., AND GUSEV, A.V. 1975. Short Term Ice Creep and Microcrack Formation Kinetics. Int. Symp. on Physics of Ice and Snow, Leningrad, 1973. Transl. from Russian. USACRREL TL 539:196-203, Hanover, N.H.